

## Article

# Anthropogenic Influences on the Hydrochemical Characteristics of the Groundwater in Xiamen City, China and Their Evolution

Zhenghong Li <sup>1,2</sup>, Jianfeng Li <sup>1,2,\*</sup>, Yuchen Zhu <sup>1,2,\*</sup>, Yasong Li <sup>1,2</sup> and Qichen Hao <sup>1,2</sup> <sup>1</sup> Fujian Provincial Key Laboratory of Water Cycling and Eco-Geological Processes, Xiamen 361000, China<sup>2</sup> Institute of Hydrogeology and Environmental Geology, CAGS, Shijiazhuang 050061, China

\* Correspondence: lijianfeng@mail.cgs.gov.cn (J.L.); zhuyuchen@mail.cgs.gov.cn (Y.Z.)

**Abstract:** This study analyzed the anthropogenic influences on the hydrochemical composition characteristics of the groundwater in Xiamen City, Fujian province, China, and their evolution. Based on the hydrochemical data of the groundwater of 1993 and 2019–2021, this study identified the indices of the anthropogenic influences using mathematical and statistical analysis methods, such as contrast coefficient, standard deviation, and Mahalanobis distance. The analytical results are summarized as follows: (1) the number of the indices affecting the groundwater quality in Xiamen increased from nine in 1993 to 15 in 2019, and the six increased indicators included  $\text{NO}_3^-$ , Pb,  $\text{NH}_4^+$ ,  $\text{Al}^{3+}$ ,  $\text{NO}_2^-$  and Cu (the contribution rates to poor-quality were 26.0%, 16.3%, 10.6%, 4.1%, 0.8% and 0.8%, respectively) which were related to the input of human activities. During this period, the number of hydrochemical types increased from 19 in 1993 to 28 in 2019, with a decrease in the water of the  $\text{HCO}_3^-$  type and an increase in the water of Cl and  $\text{SO}_4$  types; (2) In 2019,  $\text{NO}_3^-$  had higher content than  $\text{SO}_4^{2-}$  in the groundwater and became a major anion, forming the water of  $\text{NO}_3^-$  type; (2) as indicated by the analytical results obtained using the Mahalanobis distance method, areas with strong anthropogenic influences include densely populated areas and areas with intensively distributed industrial enterprises, while anthropogenic influences are very weak in the northern forest land area.

**Keywords:** evolution of hydrochemical characteristics; identification of hydrochemical anomalies; human activities; influence degree; Mahalanobis distance



**Citation:** Li, Z.; Li, J.; Zhu, Y.; Li, Y.; Hao, Q. Anthropogenic Influences on the Hydrochemical Characteristics of the Groundwater in Xiamen City, China and Their Evolution. *Water* **2022**, *14*, 3377. <https://doi.org/10.3390/w14213377>

Academic Editors: Guanxing Huang and Liangping Li

Received: 14 September 2022

Accepted: 22 October 2022

Published: 25 October 2022

**Publisher's Note:** MDPI stays neutral with regard to jurisdictional claims in published maps and institutional affiliations.



**Copyright:** © 2022 by the authors. Licensee MDPI, Basel, Switzerland. This article is an open access article distributed under the terms and conditions of the Creative Commons Attribution (CC BY) license (<https://creativecommons.org/licenses/by/4.0/>).

## 1. Introduction

Safe drinking water, which is closely related to human health, food security, and the orderly development of the social economy, is essential for the sustainable development of a city [1,2]. With the acceleration of urbanization, the area of urban built-up areas and the number and density of the urban population have increased dramatically, leading to a sharp increase in the demand for water resources [3–5]. Groundwater is the main freshwater source for industrial and agricultural production, domestic drinking, and ecological water consumption and is the only source of water supply in arid and semi-arid regions [6,7]. The groundwater quality directly affects the quality of the human living environment and human health, and the groundwater environment is controlled by various factors such as meteorology, hydrogeology, and human activities [8–12]. Urbanization in China presents a sustainable and rapid growing trend, with the urbanization rate increasing from 18.57% in 1978 to 58.52% in 2017 [13]. Moreover, the ability of human beings to transform nature is continuously enhanced, and large-scale human activities have strong influences on climate [14–16], ecological environment [17,18], soil environment [19], and groundwater environment [20–22]. Many cities around the world, especially those in arid and semi-arid regions, are facing dual water stress exerted by groundwater shortage and the deterioration of water quality [23,24].

In 1984, the Commission on Groundwater Quality under the International Association of Hydrogeologists held a symposium entitled *Impact of Agriculture on Groundwater* in

Ireland [25]. The international hydrological community has paid increasing attention to and studied the influence of human activities on the groundwater environment [24,26–31]. When the groundwater environment changes under anthropogenic influences, the hydrochemical characteristics of groundwater will also change accordingly, i.e., hydrochemical anomalies occur [32]. Since various geochemical indices frequently coexist in complex geological systems through mutual influences and constraints, the synergistic effects of various geochemical indices should be fully considered during the identification of geochemical anomalies, aiming to reduce the uncertainty of their identification performance. The multi-element geochemical anomalies can be presently identified using multiple methods, such as the hydrochemical diagrams (Durov diagram, ion ratio plot, et al.) method [33], coefficient of variation [34], affine equivariant [35], and multivariate statistical method [28]. The Mahalanobis distance is a preferred composite index used to identify multi-element geochemical anomalies. This index has been widely used in geochemical fields including geochemical prospecting and metallogenic prediction [36,37], the evaluation of geochemical anomalies of hydrocarbons [38], and the identification of geochemical anomalies of sediments [39]. However, it is rarely used in the identification of hydrochemical anomalies of groundwater.

Although Xiamen has abundant rainfall, it still suffers from a severe shortage of freshwater resources, which is a key problem restricting the sustainable economic development of the city. Groundwater accounts for only about 6% of Xiamen's urban water supply [40], indicating great potential for groundwater exploitation. Moreover, groundwater is an important supplementary and backup emergency water source of Xiamen and its quality directly affects the emergency water supply ability and water supply safety of the city. This study identified the indices of anthropogenic influences using standard deviations, calculated the contrast coefficients of these indices and the Mahalanobis distances between these contrast coefficients, and determined the intensity of anthropogenic influences on the evolution of hydrochemical characteristics of the groundwater. This study qualitatively analyzed the anthropogenic influence on the changes in the groundwater chemistry of the study area since only 172 samples were collected from the large study area. The results of this study will provide some basis for the protection of groundwater and guide the management of groundwater resources to a certain extent.

## 2. Overview of the Study Area

### 2.1. Physical Geography and Social Economy

Xiamen is located in southeastern China, with geographical coordinates of 117°53'–118°26' E and 24°23'–24°54' N. This city lies in the central portion of the west coast of the Taiwan Strait and the center of the Golden Triangle of Southern Fujian Province. It covers a total area of 1700.61 km<sup>2</sup>, including approximately 390 km<sup>2</sup> of seas, with a total coastline length of approximately 234 km. Its administrative region consists of land, seas, and islands. It generally dips to SE, with high and low hills, terraces, marine plains, and tidal flats distributed from NW to SE. Moreover, the Xiamen Island, the Gulangyu Islet, and seas lie in its south. Xiamen has a mild and humid subtropical marine monsoon climate, with an average multiyear temperature of 20.9 °C and average multiyear precipitation of 1100–2000 mm, which increases from SE to NW. Xiamen has developed water systems, a dense dendritic river network, and a runoff direction from NW to SE. The rivers in the city feature small runoff, short flows, narrow channels, and shallow riverbeds. Their water quantity varies greatly with seasons and has low sediment content. Xiamen enjoys abundant marine biological resources but lacks metal mineral resources and freshwater resources.

### 2.2. Geological and Hydrogeological Conditions

Xiamen is located in the coastal metamorphic zone of southeastern Fujian and is at the intersection of the large EW-trending Nanjing-Xiamen fault and the NES-trending Changdong-Nan'ao deep-seated fault. The exposed strata in the study area consist of the Upper Triassic Wenbinshan Formation, the Lower Jurassic Lishan and Fankeng for-

mations, the Upper Jurassic Nanyuan Formation, and Quaternary strata including the Middle Pleistocene diluvium and alluvial-proluvial strata, the Upper Pleistocene alluvial-proluvial and marine strata, the Holocene alluvial-proluvial and marine strata, and the Quaternary eluvium.

The groundwater in Xiamen mainly occurs in aquifers of unconsolidated rock pores, weathered eluvial pores and fractures, and bedrock fissures (Figure 1). The pore water of unconsolidated rocks is hosted in alluvial-proluvial and marine deposits. The pore water in alluvial-proluvial deposits is distributed in the terraces on both sides of valleys and in piedmont proluvial fans. Its aquifers consist of sands, gravels, and pebbles and have a thickness of 3–9 m and a specific yield of  $<200 \text{ m}^3/\text{d}\cdot\text{m}$  [41]. The depth of water level is 0.5–5.0 m. The pore water in marine deposits is distributed in the coastal and estuarine areas. Its aquifers consist of silty sands and medium-coarse-grained sands and have a small thickness. The pore-fissure water in weathered eluvial deposits is distributed in eluvial platforms and at piedmont slope toes. Its aquifers consist of detritus and breccias and generally have a thickness of 10–20 m and a specific yield of  $<10 \text{ m}^3/\text{d}\cdot\text{m}$ . The bedrock fissure water is distributed in the fissures and faults of bedrock in mountainous areas, with the water yield controlled by structural faults. Its water content is extremely uneven, with a specific yield of  $<10 \text{ m}^3/\text{d}\cdot\text{m}$ . The groundwater in Xiamen is primarily recharged by vertical infiltration of atmospheric precipitation and agricultural irrigation as well as the lateral flow of groundwater in bedrock mountainous areas during the rainy season. The annual average natural replenishment resource is  $1.95 \times 10^3 \text{ m}^3/\text{a}$ . The regional groundwater flows from the NW and NE to the southeast coast overall.

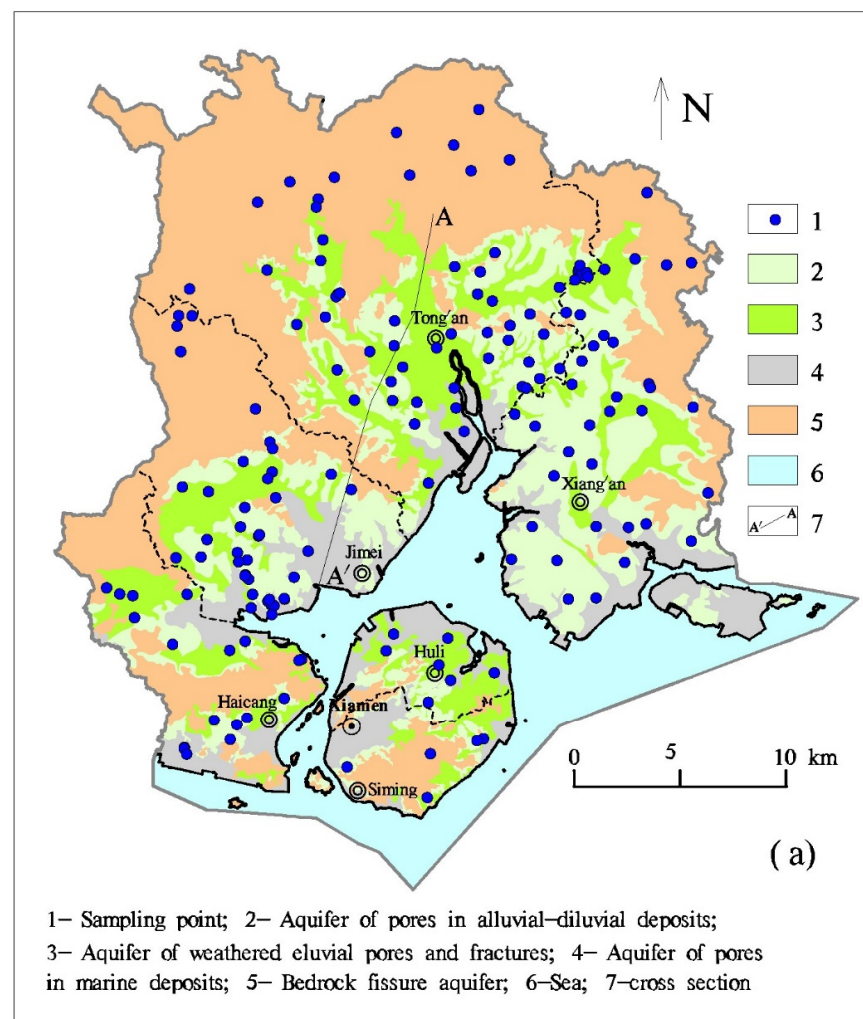
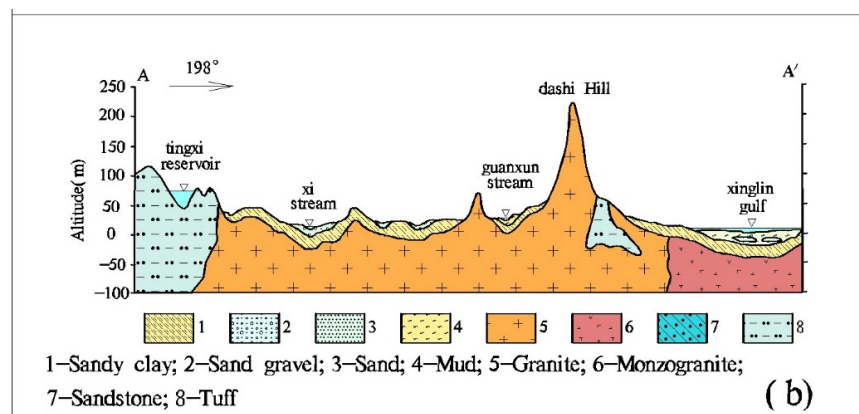


Figure 1. Cont.



**Figure 1.** Hydrogeological conditions and sampling points in Xiamen, (a) Hydrogeological conditions and sampling points; (b) Typical hydrogeological section.

### 3. Materials and Methods

#### 3.1. Data Sources

Two sets of hydrochemical data were used in this study. One set was the historical hydrochemical data of 1993 obtained from the study results of the study area. It included the data on 84 groundwater samples (19 samples of bedrock fissure water, 27 pore-fissure water samples, and 38 pore water samples), detailing the locations of sampling points, types of water-bearing media, hydrochemical types, pH, COD, the total dissolved solids (TDS) content, and the contents of  $\text{HCO}_3^-$ ,  $\text{SO}_4^{2-}$ ,  $\text{Cl}^-$ ,  $\text{K}^+\text{+Na}^+$ ,  $\text{Mg}^{2+}$ ,  $\text{NH}_4^+$ ,  $\text{NO}_2^-$ ,  $\text{NO}_3^-$ ,  $\text{F}^-$ ,  $\text{Fe}$ ,  $\text{Al}^{3+}$ ,  $\text{Cu}$ ,  $\text{Pb}$ ,  $\text{Zn}$ ,  $\text{As}$ , and  $\text{Cr}^{6+}$ . Unfortunately, the  $\text{Ca}^{2+}$  content was not recorded.

The other set of original data was 2019–2021 hydrochemical data of groundwater samples surveyed by the project team of this study. These samples were mostly collected from large-diameter wells or small pumping wells in villages and small towns, and 75% of the wells had a depth less than 50 m. The data on 172 groundwater samples were obtained in total, including 58 samples of bedrock fissure water, 72 pore-fissure water samples, and 42 pore water samples. Regarding sampling densities, seven and 8–18 samples were collected per  $100 \text{ km}^2$  in bedrock mountainous areas and plains, respectively. This set of data contained all the information that matches the historical data. Two 500 mL polyethylene bottles were used to store filtered ( $1.2\text{-}\mu\text{m}$  filter membrane) groundwater for the analysis of trace elements and major ions. The bottles were cleaned three times using the water to be sampled before sampling. The water sample in the bottle used to determine trace elements was acidized to  $\text{pH} < 2$  using nitric acid, while the water sample in the bottle used to analyze major ions was not acidized. All samples were stored at  $4^\circ\text{C}$  until laboratory procedures could be performed.

#### 3.2. Tests and Analysis

All of the water samples were sent to the Groundwater, Mineral Water and Environmental Monitoring Center of the Institute of Hydrogeology and Environmental Geology, Chinese Academy of Geological Sciences to be tested in strict accordance with GB/T5750-2006 *Standard Examination Methods for Drinking Water* and GB 8538-2016 *National Food Safety Standard—Methods for Examination of Drinking Natural Mineral Water*. Metal ions and trace elements ( $\text{K}^+$ ,  $\text{Na}^+$ ,  $\text{Mg}^{2+}$ ,  $\text{Fe}$ ,  $\text{Cu}$ ,  $\text{Pb}$ ,  $\text{Zn}$ ,  $\text{As}$ , and  $\text{Cr}^{6+}$ ) were measured using inductively coupled plasma-mass spectrometry (ICP-MS) (Agilent 7500ce ICP-MS, Tokyo, Japan).  $\text{SO}_4^{2-}$ ,  $\text{Cl}^-$ ,  $\text{NH}_4^+$ , and  $\text{NO}_3^-$  were measured using ion chromatography (IC) (Shimadzu LC-10ADvp, Japan).  $\text{NO}_2^-$  and  $\text{HCO}_3^-$  were determined using the UV spectrophotometry method, and acid-base titration method, respectively. Chemical oxygen demand (COD) and TDS content were measured using potassium dichromate titration and the gravimetric method, respectively. To ensure the accuracy and reliability of the test results, the anion-cation balance was analyzed according to the principle of ionic balance, with analysis errors

less than 5%. All chemicals were purchased from Sinopharm Chemical Reagent Co., Ltd., Shanghai, China.

### 3.3. Multivariate Statistical Method

First, the anomaly thresholds or background values were determined according to the historical hydrochemical data. The indices of both anthropogenic influences and water-rock interactions were then identified using contrast coefficients and standard deviations. Finally, the Mahalanobis distances between the multivariate contrast coefficients of the indices of anthropogenic influences were calculated to analyze the changes in hydrochemical components and determine the intensity of anthropogenic influences on the hydrochemical characteristics of groundwater.

#### 3.3.1. Identification of the Indicative Indices of Both Anthropogenic Influences and Water-Rock Interactions

Standard deviations were used to identify the indices of both anthropogenic influences and water-rock interactions.

A standard deviation (S) is the average of the distances between some data and their average, and a higher standard deviation means higher degrees of fluctuation and dispersion of a variable. The anthropogenic inputs in groundwater have a high degree of spatial dispersion. Therefore, the standard deviation was used to analyze the dispersion degree of groundwater components to determine the indices of the anthropogenic influences on the hydrochemical characteristics of groundwater. The standard deviation is expressed as:

$$S = \sqrt{\frac{1}{N} \sum_{i=1}^N (X_i - \bar{X})^2} \quad (1)$$

where S is the standard deviation; N is the number of samples;  $X_i$  is the tested value;  $\bar{X}$  is the arithmetic average.

The contrast coefficient (V) is a metric that measures the sharpness of anomalies and represents the fluctuation of the anomalies relative to the background values. To compare the anomaly intensity of a certain indicator element in different regions, the contrast coefficient can be used to eliminate the influences caused by the phenomenon that the indicator element has different background values in different regions. First, the ratio of each variable to the anomaly threshold or background value was calculated using Equation (2), and multiple variables with unequal averages were transformed into those with equal averages. The standard deviations of the contrast coefficients of various variables were then calculated and finally compared.

$$V = \frac{X_i}{T} \quad (2)$$

where V is the contrast coefficient;  $X_i$  is the tested value; T is the anomaly threshold or background value.

The anomaly threshold or background value (T) is a metric that reflects the geochemical background. The groundwater background values refer to the natural contents of physical and chemical elements in groundwater under uncontaminated conditions. However, a natural environment with no anthropogenic influence barely exists in the strict sense [42]. To analyze the anthropogenic influences on the hydrochemical characteristics of the groundwater in the study area in the past three decades, this study determined the range of background values using the quartile method based on the hydrochemical data of 1993 [43,44].

#### 3.3.2. Intensity of Anthropogenic Influences

The Mahalanobis distance (MD) is a metric that measures multivariate distance. It is used for multivariate statistics of observed objects by characterizing the distance between

the objects and their distribution center, during which covariance is considered [45]. This metric is frequently used to calculate the similarity of various indices, identify and quantify anomalies, and sometimes select representative data from a large quantity of measurement data [46]. This study analyzed the changes in hydrochemical components by calculating the Mahalanobis distances between the contrast coefficients of the indices of anthropogenic influences in order to further determine the intensity of anthropogenic influence on the hydrochemical characteristics of groundwater. The calculation formula for Mahalanobis distance is as follows:

$$D^2 = (x_i - \bar{x})S^{-1}(x_i - \bar{x})' \quad (3)$$

where  $D^2$  is the Mahalanobis distance;  $x_i$  is an index value of a sample;  $\bar{x}$  is the arithmetic average of various indices;  $S$  is the standard deviation.

This study used the Kriging interpolation method of MapGis K9 to analyze the intensity grades of anthropogenic influences on the hydrochemical characteristics of the groundwater and then plotted the map of regional anthropogenic influence intensity.

## 4. Results and Discussion

### 4.1. Characteristics of Groundwater Quality Indicators

The descriptive statistics for the indicators analyzed in groundwater samples in Xiamen City are summarized in Table 1. Among anions in the groundwater of Xiamen,  $\text{NO}_3^-$  showed the highest median concentration of 42.23 mg/L, followed by  $\text{Cl}^-$ ,  $\text{SO}_4^{2-}$  and  $\text{F}^-$ . High concentrations of  $\text{NH}_4^+$  occurred in groundwater in Xiamen, and up to 107.0 mg/L.  $\text{Na}^+$  ranged from 2.68 mg/L to 4043.8 mg/L, with the median of 32.55 mg/L. Among trace metal(loid)s in the groundwater of Xiamen, Fe showed the highest median concentration of 0.03 mg/L, followed by Zn, Pb, Cu, As,  $\text{Cr}^{6+}$  and  $\text{Al}^{3+}$ . According to the standard for groundwater quality of China (GAQSIQPRC, 2017) [47], the percent of groundwater samples with the concentrations of indicators that exceeded the allowable values (PEV) for drinking purposes are also in Table 1. In Xiamen City,  $\text{NO}_3^-$  showed the highest PEV of 22.09%, followed by Fe, Pb,  $\text{NH}_4^+$ ,  $\text{F}^-$ ,  $\text{Cl}^-$ ,  $\text{Al}^{3+}$ ,  $\text{SO}_4^{2-}$ ,  $\text{NO}_2^-$ ,  $\text{Na}^+$ , Cu, and Zn, while the PEVs of the other two indicators were zero.

**Table 1.** Descriptive statistics of concentrations of groundwater indicators.

Item	Min	Med	Max	SD	Detection Limits	Number of Non-Detects	Allowable Values	PEV (%)
$\text{SO}_4^{2-}$ (mg/L)	0.37	24.72	1171.0	107.86	0.2	0	250	1.74
$\text{Cl}^-$ (mg/L)	1.29	35.19	7073.0	548.16	0.1	0	250	2.91
$\text{NO}_3^-$ (mg/L)	0.39	42.23	2223.14	177.53	0.2	0	88.6	22.09
$\text{NO}_2^-$ (mg/L)	ND	ND	5.20	0.55	0.002	110	3.29	1.16
$\text{F}^-$ (mg/L)	ND	0.19	11.90	1.04	0.1	49	1.0	7.56
$\text{Na}^+$ (mg/L)	2.68	32.55	4034.0	305.49	0.013	0	200	1.16
$\text{NH}_4^+$ (mg/L)	ND	ND	107.0	11.45	0.04	117	0.64	9.30
$\text{Al}^{3+}$ (mg/L)	ND	ND	6.65	0.54	0.02	146	0.2	2.33
Fe (mg/L)	ND	0.03	6.76	0.72	0.02	49	0.3	13.95
Pb (mg/L)	ND	0.001	0.806	0.07	0.001	66	0.01	13.95
Cu (mg/L)	ND	ND	5.51	0.42	0.010	164	1.0	0.58
Zn (mg/L)	ND	0.01	7.74	0.60	0.002	42	1.0	0.58
As (mg/L)	ND	ND	0.009	0.001	0.001	114	0.01	0
$\text{Cr}^{6+}$ (mg/L)	ND	ND	0.017	0.002	0.004	161	0.05	0

SD = standard deviation; ND = below the limit of detection; Allowable Values = data from (GAQSIQPRC, 2017); PEV = percent of groundwater samples with the concentration of one index exceeded the allowable value.

## 4.2. Hydrochemical Changes in Groundwater

### 4.2.1. Changes in Groundwater Chemical Composition

The evaluation indices used in this study were the water quality indices specified in GB/T14848-2017 *Standard for groundwater quality*. They were contained in the hydrochemical data of 1993 and consisted of 17 indices, namely pH, COD, TDS content,  $\text{SO}_4^{2-}$ ,  $\text{Cl}^-$ ,  $\text{Na}^+$ ,  $\text{NH}_4^+$ ,  $\text{NO}_2^-$ ,  $\text{NO}_3^-$ ,  $\text{F}^-$ , Fe,  $\text{Al}^{3+}$ , Cu, Pb, Zn, As, and  $\text{Cr}^{6+}$ . We next analyzed the changes in the chemical composition of the groundwater in Xiamen in the past three decades by comparing the number and contribution rates of the influencing factors of groundwater quality between 1993 and 2019–2021.

The following evaluation results of the groundwater quality of Xiamen in the past three decades were obtained based on the number of groundwater samples: (1) the proportion of Class I to III potable groundwater decreased from 40% in 1993 to 28.5% during 2019–2021; (2) the total proportion of poor-quality and undrinkable groundwater (Class IV and V) increased from 60% in 1993 to 71.5% in 2019–2021; (3) the proportion of Class IV water that can become portable water after proper treatment increased from 28.2% in 1993 to 51.2% in 2019–2021, and the proportion of non-portable Class V water decreased from 31.8% in 1993 to 20.3% in 2019–2021 (Table 2).

**Table 2.** Comparison of the evaluation results of groundwater quality between 1993 and 2019–2021.

Year	Number of Samples	Proportion/%					Water Inferior to Class III	
		Class I	Class II	Class III	Class IV	Class V	Number of Samples	Proportion/%
1993	85	12.9	11.8	15.3	28.2	31.8	51	60.0
2019	172	1.2	4.7	22.7	51.2	20.3	123	71.5

The number of the indices affecting the groundwater quality in Xiamen increased from nine in 1993 to 15 in 2019–2021 (Figure 2). The additional six indices during 2019–2021 consisted of  $\text{NO}_3^-$ , Pb,  $\text{NH}_4^+$ ,  $\text{Al}^{3+}$ ,  $\text{NO}_2^-$ , and Cu (the contribution rates to poor-quality groundwater were 26.0%, 16.3%, 10.6%, 4.1%, 0.8% and 0.8%, respectively), among which  $\text{NO}_3^-$  and Pb had contribution rates second only to pH.

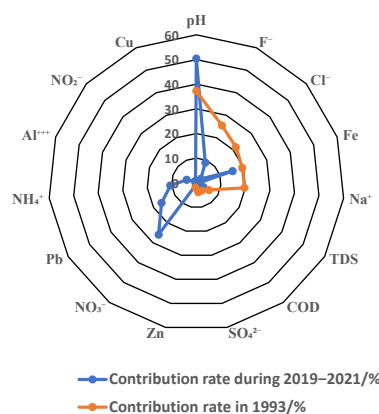


**Figure 2.** Main indices affecting groundwater quality and their contribution rates.

### 4.2.2. Changes in the Hydrochemical Types of Groundwater

Human activities have not only changed the groundwater quality but also affected and changed the natural hydrochemical field of groundwater due to a large number of anthropogenic inputs [48].

The groundwater of Xiamen had simple hydrochemical types in 1993. Specifically, 19 types were identified in 67 samples, and seven types were concentrated in 70% of the groundwater samples, namely  $\text{Na-HCO}_3$ ,  $\text{Ca-Na-HCO}_3$ ,  $\text{Na-HCO}_3\cdot\text{Cl}$ ,  $\text{Na-Ca-HCO}_3$ ,

Na·Cl, Na·Ca·HCO<sub>3</sub>·Cl, and Na·Cl·HCO<sub>3</sub>. Regarding anions, the groundwater was dominated by the HCO<sub>3</sub> type, which accounted for 46.3%; followed by the HCO<sub>3</sub>·Cl type, which accounted for 25.4%. Moreover, the groundwater of SO<sub>4</sub>·Cl and Cl·SO<sub>4</sub> types accounted for a minimum proportion of 1.5% each. In terms of cations, the groundwater in Xiamen in 1993 was dominated by Na and Na·Ca types, which accounted for 41.8% and 25.4%, respectively. They were followed by the Ca·Na type, which accounted for 14.9%. Additionally, the water of Ca, Na·Mg, Ca·Mg, Ca·Na·Mg, and Na·Mg types accounted for 1.5%–6.05% each.

The hydrochemical types of groundwater in Xiamen increased during 2019–2021 compared to 1993. Specifically, 28 hydrochemical types were identified in 172 samples, and seven hydrochemical types were concentrated in 70% of the groundwater samples, namely Ca·Na·HCO<sub>3</sub>, Na·Ca·Cl, Na·Ca·HCO<sub>3</sub>, Ca·Na·HCO<sub>3</sub>·Cl, Na·Ca·HCO<sub>3</sub>·Cl, Na·Ca·Cl·HCO<sub>3</sub>, Ca·HCO<sub>3</sub>, and Na·Ca·Cl·SO<sub>4</sub>. Regarding anions, the groundwater was still dominated by the HCO<sub>3</sub> type, whose proportion, however, decreased to 31.4%. By contrast, the Cl<sup>-</sup> and SO<sub>4</sub><sup>2-</sup> contents in the groundwater increased, with the water of Cl type and the hydrochemical types dominated by Cl (Cl·HCO<sub>3</sub>, Cl·HCO<sub>3</sub>·SO<sub>4</sub> type, and Cl·SO<sub>4</sub> types) accounted for 16.9% and 17.4%, respectively. Moreover, the proportion of the water of SO<sub>4</sub> type or types dominated by SO<sub>4</sub> increased to 5.3%. Regarding cations, the Ca<sup>2+</sup> content increased, the Mg<sup>2+</sup> content decreased, and the groundwater was dominated by the Na·Ca type, whose proportion increased to 51.2%. This type was followed by the Ca·Na type, which accounted for 36.0%. Furthermore, the water of Ca and Na types had a low proportion of 6.4% each.

Groundwater in the pore-fissure aquifer showed higher Cl<sup>-</sup> and SO<sub>4</sub><sup>2-</sup> concentrations than that in the bedrock fissure aquifers and pore aquifers (Figure 3). This may have occurred due to the greater number of industrial zones and population located in the area of the pore-fissure aquifer than in the areas of the other two types of aquifers, indicating more serious anthropogenic influences.

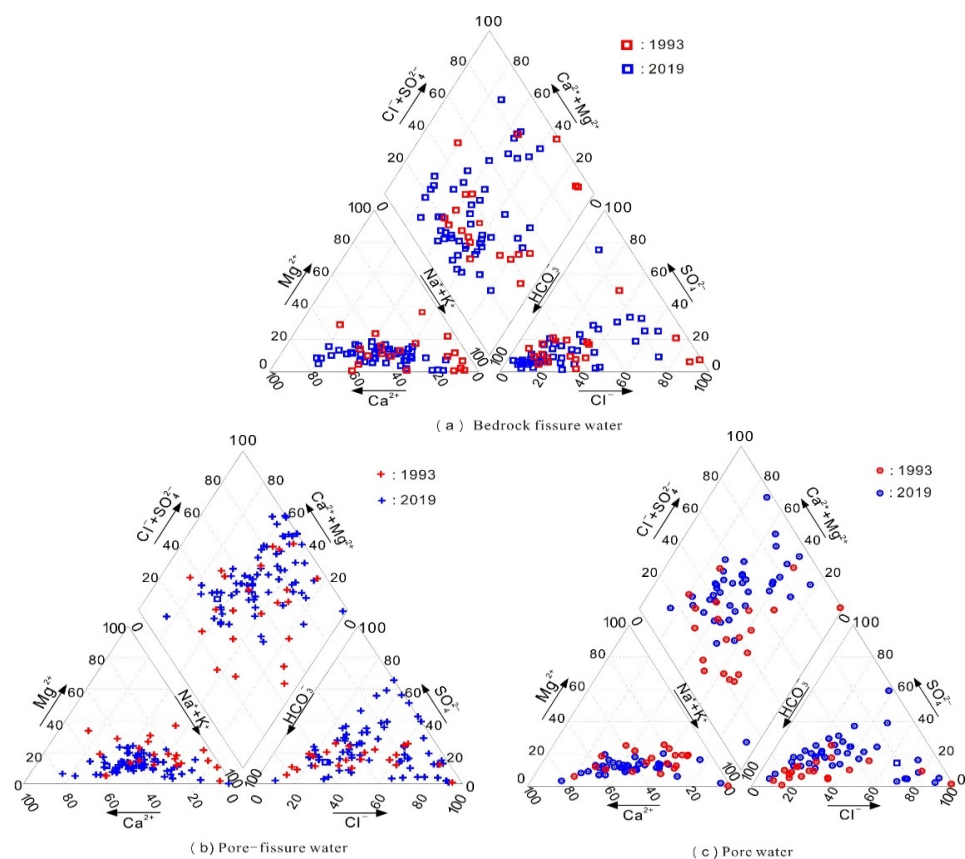


Figure 3. Piper trilinear diagrams.

The increase in the absolute content of nitrates in groundwater affects the groundwater quality, while the increase in their relative content changes the hydrochemical characteristics of groundwater. As indicated by the hydrochemical test results of the groundwater in Xiamen in 2019,  $\text{NO}_3^-$  was a major anion in Xiamen's groundwater, its relative content exceeded that of  $\text{SO}_4^{2-}$  (Table 3), and thus more water of  $\text{NO}_3^-$  type exists in the groundwater. It is known that groundwater  $\text{NO}_3^-$  in Xiamen mainly originated from anthropogenic sources, including infiltration of domestic sewage and landfill leachate [40].

**Table 3.** Characteristic parameters of the relative contents of major anions in the groundwater of Xiamen.

Item	Year	Sample Number	Range	Med	Average	SD
$\text{HCO}_3^-$	1993	45	0.9–85.8	59.9	52.2	25.6
	2019	172	0.4–89.8	35.0	36.9	24.5
$\text{SO}_4^{2-}$	1993	45	0.8–49.4	9.8	11.7	7.9
	2019	172	0.4–64.3	12.1	13.9	10.8
$\text{Cl}^-$	1993	45	6.5–97.5	21.9	31.8	23.2
	2019	172	2.8–88.2	25.7	27.3	15.9
$\text{NO}_3^-$	1993	45	0–22.5	2.5	4.3	5.1
	2019	172	0.1–84.7	20.2	21.8	16.8

#### 4.3. Anthropogenic Influences on the Hydrochemical Characteristics of Groundwater

##### 4.3.1. Indicative Indices of the Anthropogenic Influences

###### Determination of the Background Values of Groundwater in Different Water-Bearing Media

This study statistically analyzed the data of 1993, obtaining the background values of the groundwater environment in aquifers of bedrock fissures, weathered pores and fissures, and pores in alluvial-proluvial deposits, respectively (Table 4). Furthermore, the background values of indices Cu, Pb, As, and  $\text{Cr}^{6+}$  were determined to be 0, since there were a few samples of these indices and they were not detected in the water of various water-bearing media.

###### Identification of the Indicative Indices of Anthropogenic Influences

To conduct a multivariate contrast, various variables were normalized first. In other words, the upper limits of the background values of various indices in Table 3 were used as the anomaly threshold or background value (T) to calculate the contrast coefficients (V) and the standard deviations of various indices of the groundwater of Xiamen in 2019.

Anthropogenic inputs in groundwater generally have high degrees of spatial dispersion and fluctuation [48]. Therefore, standard deviations can be used to distinguish between groundwater components originating from anthropogenic inputs and those from water-rock interactions. The contrast coefficients of pH and  $\text{HCO}_3^-$  had a standard deviation of 0.09 and 0.53, respectively, indicating very weak anthropogenic influences. By contrast, the contrast coefficients of  $\text{Cl}^-$ ,  $\text{NO}_3^-$ , and  $\text{NH}_4^+$  had a standard deviation of 18.86, 35.83, and 42.76, respectively, indicating very strong anthropogenic influences. The standard deviations of the contrast coefficients of the 15 indices decreased in the order of pH,  $\text{HCO}_3^-$ , COD, total hardness, Zn, Fe,  $\text{NO}_2^-$ ,  $\text{SO}_4^{2-}$ ,  $\text{F}^-$ , TDS,  $\text{Mg}^{2+}$ ,  $\text{K}^+$ + $\text{Na}^+$ ,  $\text{Cl}^-$ ,  $\text{NO}_3^-$ , and  $\text{NH}_4^+$ . These 15 indices in the groundwater were divided into four categories according to their sources determined by the standard deviations of their contrast coefficients, as shown in Table 5.

**Table 4.** Background values of groundwater environment in different water-bearing media in Xiamen.

Item	Background Value Scope	Bedrock	Weathered	Pore Water in
		Fissure Water	Pore Fissure Water	Alluvial Proluvial Deposits
pH		6.57–7.04	6.42–6.93	6.05–7.09
COD		0.41–1.32	0.90–1.22	0.57–1.33
Cl <sup>-</sup>		12.0–28.54	27.81–76.09	14.45–76.60
SO <sub>4</sub> <sup>2-</sup>		6.05–23.54	18.97–40.71	5.64–42.81
HCO <sub>3</sub> <sup>-</sup>		44.39–102.49	38.04–218.15	43.17–166.0
NO <sub>2</sub> <sup>-</sup>		0.004–0.048	0.021–0.188	0–0.026
NO <sub>3</sub> <sup>-</sup>		0.50–4.73	6.38–29.38	2.28–13.90
F <sup>-</sup>		0.04–0.20	0.04–0.20	0.04–0.20
K <sup>+</sup> +Na <sup>+</sup>		18.05–41.32	30.36–114.59	17.94–70.61
Mg <sup>2+</sup>		1.32–5.43	4.18–17.63	2.19–6.77
NH <sub>4</sub> <sup>+</sup>		0.02–0.18	0.03–0.28	0.01–0.10
Fe		0.09–1.20	0.03–0.31	0.03–0.08
Al <sup>3+</sup>		0–0.026	0–0.037	0
Zn		0.048–0.441	0.019–0.390	0.022–0.350
TDS		96.12–251.79	180.4–379.55	124.9–337.78

**Table 5.** Standard deviations of the contrast coefficients of indices and their indicative significance.

Index	Standard Deviations	Sources	Anthropogenic Influence Intensity
pH, HCO <sub>3</sub> <sup>-</sup>	≤1	Water-rock interactions	Very weak
COD, total hardness, Zn, Fe, NO <sub>2</sub> <sup>-</sup> , SO <sub>4</sub> <sup>2-</sup> , F <sup>-</sup> , and TDS content	1–5	Water-rock interactions, supplemented by anthropogenic inputs	Weak
Mg <sup>2+</sup> , K <sup>+</sup> +Na <sup>+</sup>	5–10	Anthropogenic inputs, supplemented by water-rock interactions	Strong
Cl <sup>-</sup> , NO <sub>3</sub> <sup>-</sup> , NH <sub>4</sub> <sup>+</sup>	>10	Anthropogenic inputs	Very strong

#### 4.3.2. Anthropogenic Influence Intensity

The Mahalanobis distance is a metric used for multivariate statistics of observed objects. This study combined five indices: Mg<sup>2+</sup>, K<sup>+</sup>+Na<sup>+</sup>, Cl<sup>-</sup>, NO<sub>3</sub><sup>-</sup>, and NH<sub>4</sub><sup>+</sup> subject to strong or very strong anthropogenic influences combined into a whole, then calculated the Mahalanobis distances of the contrast coefficients of various groundwater samples collected in 2019, and finally analyzed the anthropogenic influence intensity of various samples. Figure 4 shows the distribution of the Mahalanobis distances of 172 samples. The anthropogenic influence intensity of these samples was divided into four grades according to the Mahalanobis distances 0.25, 0.6, and 6 at inflexion points, which represented the boundaries of anthropogenic influence intensity grades 2, 3, and 4, respectively.

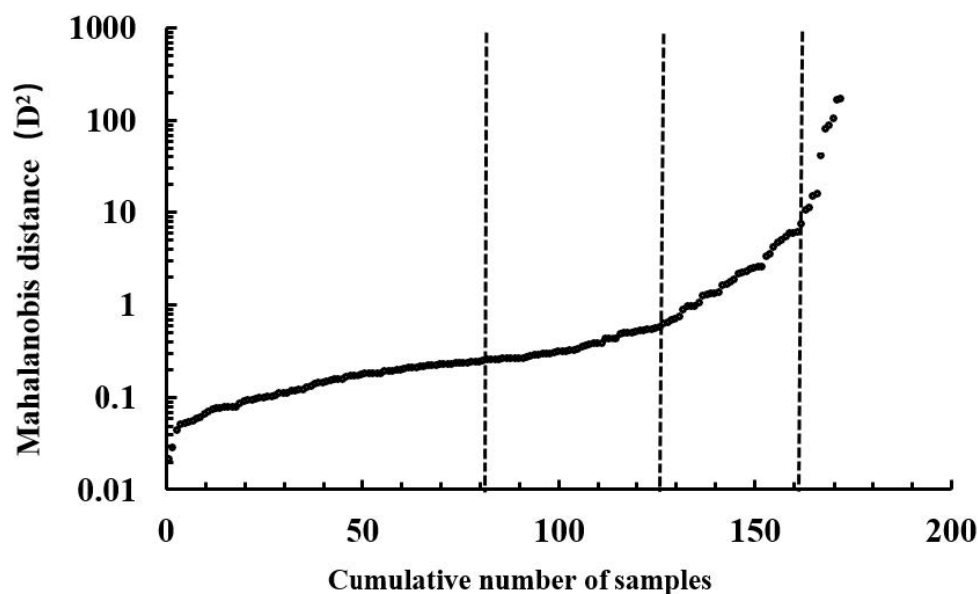


Figure 4. Mahalanobis distances of contrast coefficients of groundwater samples in 2019.

The intensity of anthropogenic influences on the hydrochemical composition of the groundwater in Xiamen was analyzed based on the Mahalanobis distance method. Figure 5 shows the types of land use and the intensity and distribution of anthropogenic influences on the hydrochemical composition of the groundwater in Xiamen. According to this figure, the groundwater subject to strong or relatively strong anthropogenic influences is mostly distributed on artificial surfaces and cultivated land, while the anthropogenic influences on the groundwater sites in forest land areas were mostly rated as weak.

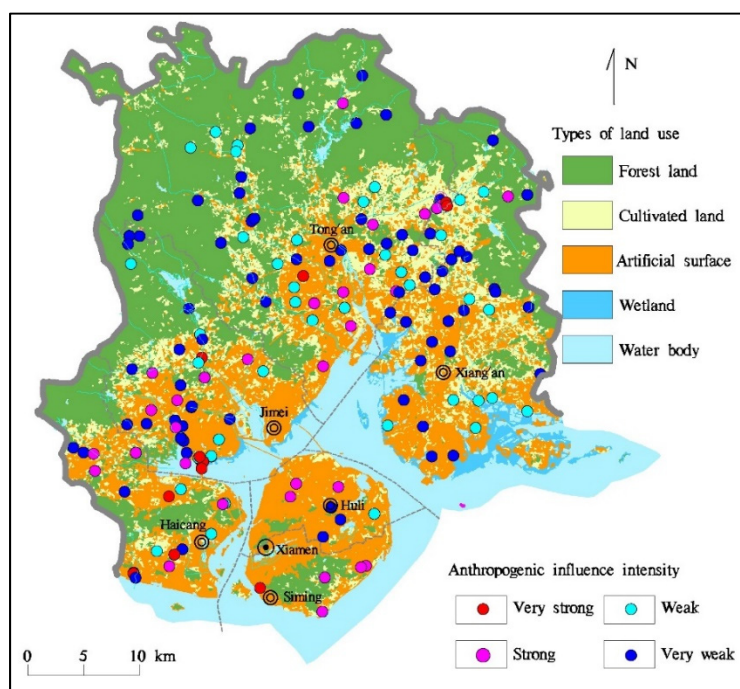
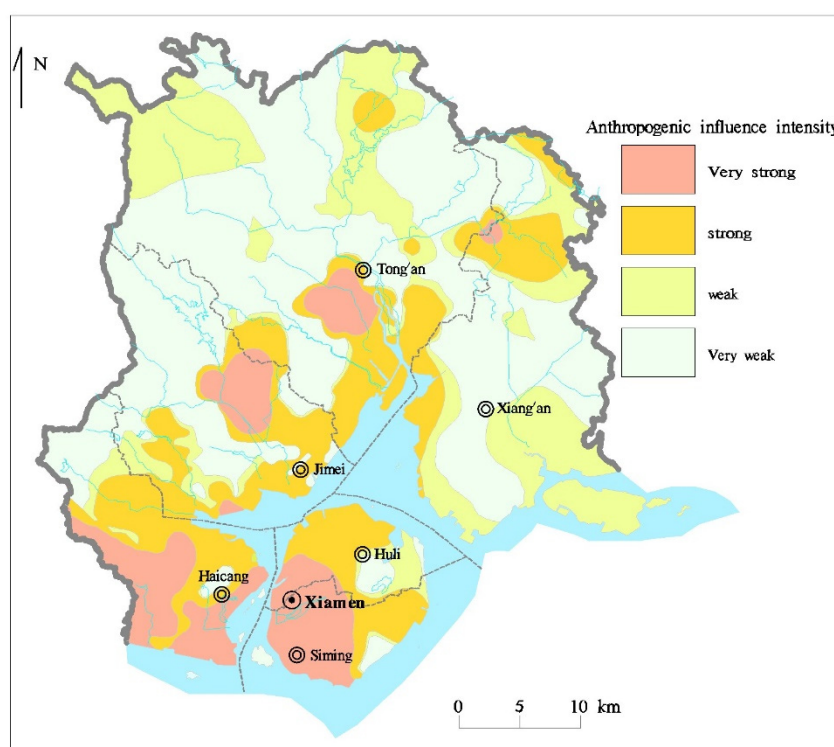


Figure 5. Map showing the distribution of the intensity of anthropogenic influences on groundwater.

Interpolation was conducted for the calculated Mahalanobis distances using the Kriging interpolation method of the MapGIS software. The anthropogenic influence intensity was then divided into four grades according to the interpolated Mahalanobis distances, obtaining the map showing the zones of the anthropogenic influence intensity (Figure 6).

According to this map, the zones subject to very strong anthropogenic influences include densely populated areas and areas with intensively distributed industrial enterprises, such as Xinxu Town in the Xiang'an District, Xike Street in the Tong'an District, Houxi Town and Xinglin Street in the Jimei District, Haicang Street in the Haicang District, and Dianqian Street in the Huli District. With low population density and high vegetation coverage, the northern bedrock mountainous area is a zone with very weak anthropogenic influences on groundwater.



**Figure 6.** Map showing the zones of the intensity of anthropogenic influences on groundwater.

## 5. Conclusions

1. The number of indices affecting the groundwater quality in Xiamen increased from nine in 1993 to 15 in 2019, and the six increased indicators included  $\text{NO}_3^-$ , Pb,  $\text{NH}_4^+$ ,  $\text{Al}^{3+}$ ,  $\text{NO}_2^-$  and Cu. The number of hydrochemical types increased from 19 in 1993 to 28 in 2019. Moreover, the water of the  $\text{HCO}_3$  type has decreased, while the water of the Cl type (including types dominated by Cl) and the  $\text{SO}_4$  type (including types dominated by  $\text{SO}_4$ ) have increased, indicating that human activities are the powerful force driving the change in groundwater chemistry in Xiamen City.
2. The increase in the relative contents of nitrates in the groundwater has changed the hydrochemical characteristics of the groundwater. Both the maximum and average relative content of  $\text{NO}_3^-$  exceed those of  $\text{SO}_4^{2-}$ . Therefore,  $\text{NO}_3^-$  has become a major anion affecting the hydrochemical nomenclature of the groundwater in Xiamen, forming the water of  $\text{NO}_3$  type (according to Shukarev classification and Designation rules).
3. As indicated by the analysis results of Mahalanobis distances, zones with very strong anthropogenic influences on groundwater include Houxi Town in Jimei District and Haicang Street in Haicang District, while zones with very weak anthropogenic influences on groundwater include the northern bedrock mountainous area. These results are consistent with the land use, industrial layout, and population distribution of Xiamen, indicating that the Mahalanobis distance method can be used to identify the hydrochemical anomalies of groundwater and determine the intensity of anthropogenic influences on groundwater and that the evaluation results obtained using this method is reasonable.

**Author Contributions:** Conceptualization, Z.L. and J.L.; methodology, Z.L.; software, Y.Z.; validation, Z.L., Y.Z. and Q.H.; formal analysis, Z.L. and J.L.; investigation, Z.L. and Y.Z.; resources, Y.L.; data curation, Z.L. and Q.H.; writing—original draft preparation, Z.L. and J.L.; writing—review and editing, J.L. and Y.L.; visualization, J.L.; supervision, Y.Z.; project administration, Z.L. and Y.Z.; funding acquisition, Z.L. All authors have read and agreed to the published version of the manuscript.

**Funding:** This study was financially supported by China Geological Survey’s project (Grant No. DD20190303 and DD20221773).

**Institutional Review Board Statement:** Not applicable.

**Informed Consent Statement:** Not applicable.

**Data Availability Statement:** The data presented in this study are available on request from the corresponding author.

**Conflicts of Interest:** The authors declare no conflict of interest.

## References

1. Wang, Y.; Zheng, C.; Ma, R. Review: Safe and sustainable groundwater supply in China. *Appl. Hydrogeol.* **2018**, *26*, 1301–1324. [[CrossRef](#)]
2. Turhan, A.; Ozmen, N. Influence of Chloride on Growth, Fruit Yield and Quality Parameters of Processing Pepper. *J. Agric. Nat.* **2021**, *24*, 1139–1144.
3. Döll, P.; Müller Schmied, H.; Schuh, C.; Portmann, F.T.; Eicker, A. Global-scale assessment of groundwater depletion and related groundwater abstractions: Combining hydrological modeling with information from well observations and GRACE satellites. *Water Resour. Res.* **2014**, *50*, 5698–5720. [[CrossRef](#)]
4. Mirdashtvan, M.; Najafinejad, A.; Malekian, A.; Sadoddin, A. Sustainable water supply and demand management in semi-arid regions: Optimizing water resources allocation based on RCPs scenarios. *Water Resour. Manag.* **2021**, *35*, 5307–5324. [[CrossRef](#)]
5. Liu, C.L.; Zheng, J.H.; Li, Z.H.; Li, Y.S.; Hao, Q.C.; Li, J.F. Analysis on the situation and countermeasures of water resources supply and demand in the cities of small and medium-sized river basins along southeast coast of China-taking Xiamen City as an example. *J. Groundw. Sci. Eng.* **2021**, *9*, 350–358.
6. Yang, H.F.; Meng, R.F.; Li, W.P.; Li, Z.Y.; Zhi, C.S.; Bao, X.L.; Li, C.Q.; Liu, F.T.; Wu, H.P.; Ren, Y. Groundwater resources of the Haihe River Basin and its development potential. *Geol. China* **2021**, *48*, 1032–1051.
7. Nasiri, S.; Ansari, H.; Ziaei, A.N. Determination of water balance equation components in irrigated agricultural watersheds using SWAT and MODFLOW models: A case study of Samalqan plain in Iran. *J. Groundw. Sci. Eng.* **2022**, *10*, 44–56.
8. Zhang, Y.L.; Ma, R.; Li, Z.H. Human health risk assessment of groundwater in Hetao Plain (Inner Mongolia Autonomous Region, China). *Environ. Monit. Assess.* **2014**, *186*, 4669–4684. [[CrossRef](#)]
9. Tirkey, P.; Bhattacharya, T.; Chakraborty, S.; Baraik, S. Assessment of groundwater quality and associated health risks: A case study of Ranchi city, Jharkhand, India. *Groundw. Sustain. Dev.* **2017**, *5*, 85–100. [[CrossRef](#)]
10. Adimalla, N.; Wu, J. Groundwater quality and associated health risks in a semi-arid region of south India: Implication to sustainable groundwater management. *Hum. Ecol. Risk Assess. Int. J.* **2019**, *25*, 191–216. [[CrossRef](#)]
11. Adimalla, N. Controlling factors and mechanism of groundwater quality variation in semiarid region of South India: An approach of water quality index (WQI) and health risk assessment (HRA). *Env. Geochem. Health* **2020**, *42*, 1725–1752. [[CrossRef](#)] [[PubMed](#)]
12. Egbi, C.D.; Anornu, G.K.; Ganyaglo, S.Y.; Appiah-Adjei, E.K.; Li, S.L.; Dampare, S.B. Nitrate contamination of groundwater in the lower volta river basin of Ghana: Sources and related human health risks. *Ecotoxicol. Environ. Saf.* **2020**, *191*, 110227. [[CrossRef](#)]
13. Li, X.Y.; Zhang, Y.L.; Li, Z.H.; Wang, R. Response of the groundwater environment to rapid urbanization in Hohhot, the provincial capital of western China. *J. Hydrol.* **2021**, *603*, 127033. [[CrossRef](#)]
14. Mote, T.; Lacke, M.; Shepherd, J.M. Radar signatures of the urban effect on precipitation distribution: A case study for Atlanta, Georgia. *Geophys. Res. Lett.* **2007**, *34*, L20710. [[CrossRef](#)]
15. Salerno, F.; Gaetano, V.; Gianni, T. Urbanization and climate change impacts on surface water quality: Enhancing the resilience by reducing impervious surfaces. *Water Res.* **2018**, *144*, 491–502. [[CrossRef](#)] [[PubMed](#)]
16. Zhou, Q.Q.; Leng, G.Y.; Su, J.H.; Ren, Y. Comparison of urbanization and climate change impacts on urban flood volumes: Importance of urban planning and drainage adaptation. *Sci. Total Environ.* **2019**, *658*, 24–33. [[CrossRef](#)]
17. Ariken, M.; Zhang, F.; Liu, K.; Fang, C.L.; Kung, H.T. Coupling coordination analysis of urbanization and eco-environment in Yanqi Basin based on multi-source remote sensing data. *Ecol. Indic.* **2020**, *114*, 106331. [[CrossRef](#)]
18. Yu, B.B. Ecological effects of new-type urbanization in China. *Renew. Sustain. Energy Rev.* **2021**, *135*, 110239. [[CrossRef](#)]
19. Shaharoon, B.; Al-Ismaily, S.; Al-Mayahi, A.; Al-Harrasi, N.; Al-Kindi, R.; Al-Sulaimi, A.; Al-Busaidi, H.; Al-Abri, M. The role of urbanization in soil and groundwater contamination by heavy metals and pathogenic bacteria: A case study from Oman. *Heliyon* **2019**, *5*, e01771. [[CrossRef](#)]

20. Li, Z.H.; Zhang, Y.L.; Hu, B.; Wang, L.J.; Zhu, Y.C.; Li, J.F. Driving action of human activities on NO<sub>3</sub>—N pollution in confined groundwater of Togtoh County, Inner Mongolia. *Acta Geosci. Sinica* **2018**, *39*, 358–364.
21. Kaur, L.; Rishi, M.S.; Siddiqui, A.U. Deterministic and probabilistic health risk assessment techniques to evaluate non-carcinogenic human health risk (NHHR) due to fluoride and nitrate in groundwater of Panipat, Haryana, India. *Environ. Pollut.* **2020**, *259*, 113711. [[CrossRef](#)] [[PubMed](#)]
22. Zhu, L.; Yang, M.N.; Zhang, Y.X.; Liu, J.T. Research on distribution and influence factor of nitrate of shallow groundwater in Dongsheng and surrounding area. *J. Water Resour. Water Eng.* **2016**, *27*, 37–41,45.
23. Kangabam, R.D.; Bhoominathan, S.D.; Kanagaraj, S.; Govindaraju, M. Development of a water quality index (WQI) for the Loktak Lake in India. *Appl. Water Sci.* **2017**, *7*, 2907–2918. [[CrossRef](#)]
24. Cheng, X.; Chen, L.D.; Sun, R.H.; Jing, Y.C. Identification of regional water resource stress based on water quantity and quality: A case study in a rapid urbanization region of China. *J. Clean. Prod.* **2019**, *209*, 216–223. [[CrossRef](#)]
25. Aldwell, C.R. Agriculture and groundwater must co-exist. *Environ. Geol. Water Sci.* **1986**, *9*, 1–2. [[CrossRef](#)]
26. Wang, Y.X.; Ma, T.; Guo, Q.H.; Ma, R. Groundwater and environmental change. *Earth Sci. Front.* **2005**, *12*, 14–21.
27. Wang, J.Z.; Zhang, G.H.; Nie, Z.L.; Yan, M.J.; Wang, Y. Disturbing degree of mankind activities to groundwater in the Hutuo River Valley area. *Bull. Soil Water Conserv.* **2010**, *30*, 65–69.
28. Liu, L.; Zhou, X.; Ye, Y.H. Screening of characteristic indexes for shallow groundwater influenced by human activities using multivariate statistics. *Resour. Surv. Environ.* **2014**, *35*, 305–310.
29. Ouyang, Q.C.; Lin, B.Q.; Chen, X.W. Effects of landuse changes on hydrological processes: An analysis based on SWAT model. *J. Subtrop. Resour. Environ.* **2016**, *11*, 65–70.
30. Malki, M.; Bouchaou, L.; Hirich, A.; Brahim, Y.; Choukr-Allah, R. Impact of agricultural practices on groundwater quality in intensive irrigated area of Chtouka-Massa, Morocco. *Sci. Total Environ.* **2017**, *574*, 760–770. [[CrossRef](#)]
31. Flem, B.; Reimann, C.; Fabian, K.; Birke, M.; Filzmoser, P.; Banks, D. Graphical statistics to explore the natural and anthropogenic processes influencing the inorganic quality of drinking water, ground water and surface water. *Appl. Geochem.* **2018**, *88*, 133–148. [[CrossRef](#)]
32. Zhang, X.W.; He, J.T.; Peng, C.; Zhang, C.Y.; Ni, Z.H. Comparison of identification methods of main component hydrochemical anomalies in groundwater: A case study of Liujiang Basin. *Environ. Sci.* **2017**, *38*, 3225–3234.
33. Peng, C.; He, J.T.; Liao, L.; Zhang, Z.G. Research on the influence degree of human activities on groundwater quality by the method of geochemistry: A case study from Liujiang Basin. *Earth Sci. Front.* **2017**, *24*, 321–331.
34. Zhao, W.; Lin, J.; Wang, S.F.; Liu, J.L.; Chen, Z.R.; Kou, W.J. Influence of human activities on groundwater environment based on coefficient variation method. *Environ. Sci.* **2013**, *34*, 1277–1283.
35. Rocke, D.M.; Woodruff, D.L. Identification of outliers in multivariate data. *J. Am. Stat. Assoc.* **1996**, *91*, 1047–1061. [[CrossRef](#)]
36. Ji, H.J. Multivariate method for distinguishing geochemical background from geochemical anomalies. *J. Chang. Univ. Earth Sci.* **1988**, *18*, 311–320.
37. Tian, L.M. *Geochemical Data Processing and Targets Optimization in Eastern Kunlun Orogenic Belt, Qinghai Province*; Wuhan China University of Geosciences: Wuhan, China, 2017.
38. Tang, Y.P.; Liu, Y.L. The Application of Markov distance method to the anomaly Appraisal in oil-gas geochemical prospecting. *Geophys. Geochem. Explor.* **1998**, *22*, 231–233.
39. Chen, X.N.; Wang, L.J.; Wang, H.P. Application of Mahalanobis distance anomaly in geochemical survey: Taking the 1:25000 geochemical survey of somewhere in Dulan County, Qinghai province as an example. *J. Chongqing Univ. Technol. Nat. Sci.* **2018**, *11*, 115–120.
40. Li, Z.H.; Li, Y.S.; Hao, Q.C.; Li, J.F.; Zhu, Y.C. Characteristics, genesis and treatment measures of NO<sub>3</sub>-type groundwater in Xiamen, Fujian Province. *Geol. China* **2021**, *48*, 1441–1452.
41. Li, Y.S.; Liu, C.L.; Hao, Q.C. *Report on Comprehensive Geological Survey of Xiamen-Zhangzhou-Quanzhou City*; Chinese Academy of Geological Sciences, The Institute of Hydrogeology and Environmental Geology: Shijiazhuang, China, 2021. (In Chinese)
42. Qiu, H.X.; Huang, Q.Z. The concept of groundwater environment background and its determination. *J. Ocean. Univ. Qingdao* **1994**, 16–19.
43. Helsel, D.R. Less than obvious: Statistical treatment of data below the detection limit. *Environ. Sci. Technol.* **1990**, *24*, 1767–1774. [[CrossRef](#)]
44. Lee, L.; Helsel, D. Baseline models of trace elements in major aquifers of the United States. *Appl. Geochem.* **2005**, *20*, 1560–1570. [[CrossRef](#)]
45. Song, Y.H.; Li, Z.X.; Sun, L.H.; Jia, D.C.; Bu, X.J. Contrast between Mahalanobis distance and euclidean distance in geochemical exploration processing. *Jinlin Geol.* **2008**, *27*, 117–120.
46. Jouan-Rimbaud, D.; Massart, D.L.; Saby, C.A.; Puel, C. Characterisation of the representativity of selected sets of samples in multivariate calibration and pattern recognition. *Anal. Chim. Acta* **1997**, *350*, 149–161. [[CrossRef](#)]
47. *General Administration of Quality Supervision Inspection and Quarantine of the People's Republic of China (GAQSIPRC)*; Standard for Groundwater Quality. Standards Press of China: Beijing, China, 2017.
48. Cheng, D.H.; Chen, H.H.; He, J.T.; Lin, J.; Yang, D.G.; Yu, H. A study of indicators of anthropogenic influence and water-rock interaction in groundwater system in the urban region of Beijing. *Hydrogeol. Eng. Geol.* **2007**, *34*, 37–42.